



## Equilibrium, kinetic and thermodynamic studies on the removal of reactive dye RBBR using discarded SBS paperboard coated with PET as an adsorbent

Karine Thaise Rainert<sup>a</sup>, Hayssa Carolini Alamar Nunes<sup>a</sup>, Marcel Jefferson Gonçalves<sup>b</sup>, Lorena Benathar Ballod Tavares<sup>a,\*</sup>

<sup>a</sup>Regional University of Blumenau, Environmental Engineering Postgraduate, Laboratory of Biomass Engineering, 89030-000, Blumenau, SC, Brazil, Tel. +55 4732216077; emails: lorena@furb.br (L.B.B. Tavares), krainert@furb.br (K.T. Rainert), yssa.nunes@gmail.com (H.C.A. Nunes)

<sup>b</sup>Regional University of Blumenau, Department of Chemical Engineering, 89030-000, Blumenau, SC, Brazil, email: marcelg@furb.br

Received 10 February 2017; Accepted 7 August 2017

### ABSTRACT

A waste material in the form of discarded solid bleached sulfate (SBS) paperboard coated with polyethylene terephthalate (PET) was characterized by Fourier transform infrared spectroscopy and scanning electron microscopy. The aim was to investigate its use as an adsorbent for the removal of the reactive dye Remazol Brilliant Blue R (RBBR) from aqueous solutions in batch mode. The effects of pH, agitation speed and adsorbent dosage were determined using the response surface methodology. Sorption of RBBR onto SBS paperboard coated with PET was found to be efficient at pH 2. The optimum conditions were adsorbent dose of 4.5 g and agitation speed of 100 rpm. With regard to the kinetics, four different isotherm models were tested and the pseudo-second-order model best described the sorption mechanism ( $R^2 = 0.999$ ). The equilibrium data were analyzed using Freundlich, Langmuir, Temkin and Dubinin–Radushkevich isotherms. The Freundlich adsorption capacity ( $Q_e$ ) was found to be 1.21 mg g<sup>-1</sup> with  $R^2 = 0.995$ . Thermodynamic studies showed a negative  $\Delta H^\circ$  value, indicating that the sorption process is exothermic.

*Keywords:* Textile dye; Adsorption; Experimental design

### 1. Introduction

The dyeing and finishing processes applied in the textile industry are large generators of wastewaters, consisting of organic and inorganic fillers, strong color, high biochemical oxygen demand and chemical oxygen demand, and suspended particles [1,2]. The dyes present in these wastewaters, even at low concentrations, can have a serious impact on the aquatic environment and public health due to their potentially carcinogenic, toxic and mutagenic nature [3,4]. Many of these dyes are of synthetic origin and have complex aromatic structures that make them more stable and resistant to fading in the presence of light, high temperature and chemicals, thus hindering their degradation [5].

Reactive dyes are among the more commonly applied dyes since they have a chromophore group and a functional group that can form covalent bonds with cellulosic fibers [6]. Remazol Brilliant Blue R (RBBR) is an example of a reactive dye that is highly resistant to degradation, due to its anthraquinone structure, and thus it remains longer in the wastewater [5]. RBBR also has a relatively low binding capacity (75%–80%) to bind to fabric, due to the formation of vinyl sulfone and hydrolysis reactions. Furthermore, RBBR is an anthracene derivative, it represents an important class of recalcitrant organopollutants and it is toxic [7,8]. Thus, the development of a strategy to eliminate this dye and reduce its effect on natural water bodies is of great importance [9].

Due to the wide diversity and the complexity of wastewaters, together with the requirements imposed by government legislation regarding effective treatments, new

\* Corresponding author.

technologies have been developed seeking to improve the existing treatment processes, in terms of cost, time and efficiency, for the elimination of the toxicity of wastewaters [1]. There are several types of wastewater treatments, which can involve physical, chemical and biological processes, including flocculation, adsorption, oxidation, filtration, coagulation and electrochemistry [10]. Among the various physical and chemical methods, the adsorption process is one of the most effective techniques for removing color from wastewaters [2,5,11].

Currently, three dye adsorption mechanisms have been recognized. The first is based on dispersion forces between the  $\pi$  electrons of the aromatic ring and the  $\pi$  electrons in the adsorbent layer. The  $\pi$ - $\pi$  interactions are enhanced when adsorption occurs in the smaller micropore because the potential for adsorption is enhanced by the proximity between the pore walls. The second mechanism involves the interaction between the electron donor groups on the surface of the adsorbent and the aromatic ring that acts as a receiver. This kind of interaction occurs in larger micropores and mesopores. The third mechanism is based on the formation of a hydrogen bond between the hydroxyl aromatic group and surface oxygen groups that are mainly located on the external surface or edges of the layers of adsorbent [12].

However, one of the main disadvantages associated with adsorption processes is the high cost of activated carbon adsorbents and the large amount of waste produced at the end of the procedure [4]. Thus, there is growing interest in the use of biosorbents derived from lignocellulosic waste, or industrial, agricultural and other natural waste materials, as potential adsorbents for scavenging different varieties of toxic pollutants [13]. The various adsorbents studied for the removal of textile dyes and heavy metal ions from aqueous media include coconut kernels [14], nanocomposites [15–19], hen feathers [13], egg shell, egg shell membrane [20], *Hibiscus cannabinus* fiber [21], coconut shells [6], rice husk [22], peach gum [23], leaves of *Azadirachta indica* [24], sugarcane bagasse [25] corncobs [26], 'De-Oiled Soya' and 'Bottom Ash' [27].

These wastes are good adsorbents and can generally be used after minimal processing, thereby reducing the production costs, representing a low-cost raw material and eliminating the energy costs associated with heat treatment [28]. Another example of lignocellulosic waste material that can be applied for this purpose is solid bleached sulfate (SBS) paperboard coated with polyethylene terephthalate (PET), referred to herein as SBS/PET board. It has been reported that the PET present in this waste material is an adsorbent of organic compounds such as dyes and phenols [12]. SBS/PET board has increasingly been used for food packaging purposes due to the changing eating habits of consumers caused by urbanization and globalization. These new habits include the prioritization of foods that are easier and quicker to prepare, boosting the industrial development of semi-ready-to-eat and ready-to-eat foods [29,30].

However, the production of SBS/PET board, used as packaging for these types of food products, generates large amounts of solid waste that has a negative impact on the environment. Thus, studies on the reuse of this type of packaging waste are of environmental significance, as this will decrease the volume discarded to landfills. In this context, the aims of this study were: first, to reduce waste generation by investigating the reuse of discarded SBS/PET board originating from the

packaging industry as an industrial waste of lignocellulosic origin; and, second, to develop a sustainable adsorption process for the treatment of wastewaters containing dyes. Hence, this paper reports the results of an investigation on the adsorption of the textile dye RBBR, using as a sorbent material discarded pieces of SBS paperboard coated with PET. Kinetic, isotherm and thermodynamic studies were conducted to understand the nature and mechanism of the adsorption process.

## 2. Materials and methods

### 2.1. Materials

The reactive dye RBBR was provided by M/s DyStar (Brazil) and used as an adsorbate model due to its wide application in the textile industry. The molecular structure of RBBR is shown in Fig. 1. The SBS/PET board employed in this study is used in the thermoforming of food packaging and was provided by M/s Baumgarten Gráfica (Blumenau, Brazil) as a waste material. It was processed in a slicer to reduce the size to around 7 mm.

### 2.2. Characterization of adsorbent

#### 2.2.1. FTIR spectrometry

Fourier transform infrared (FTIR) spectrometric analysis was performed on a Bruker spectrometer (model Vertex 70) in order to identify the functional groups on the surface of the SBS/PET board waste material with and without the dye.

#### 2.2.2. Scanning electronic microscopy

The morphology of the SBS/PET board was investigated by scanning electron microscopy (SEM) using a TESCAN microscope (model VEJA 3).

#### 2.2.3. Determining the point of zero charge

The point of zero charge (PZC) of the SBS/PET board was determined using a 0.01 M NaCl solution, adjusting the pH in the range of 1–12 using NaOH or HCl (0.01 M). The SBS/PET board (30 mg) was placed in Erlenmeyer flasks with 10 mL of 0.01 M NaCl at different pH values. These flasks were kept under stirring at 150 rpm for 24 h at 30°C. After this period, the pH was measured again. To determine the PZC (when the  $\Delta\text{pH}$  of the solution is equal to zero), a graph was constructed using the value  $\Delta\text{pH}$  vs. the  $\text{pH}_{\text{initial}}$  [31].

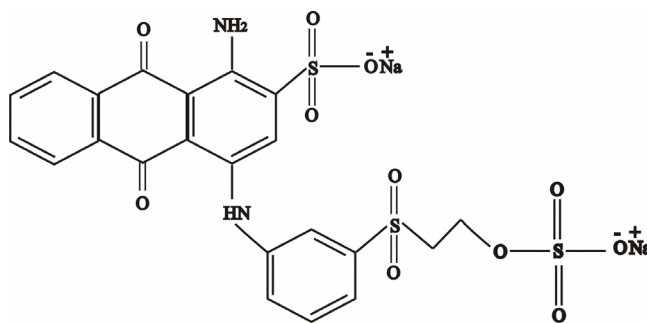


Fig. 1. Chemical structure of RBBR.

### 2.3. Adsorption study

A  $3^k$  factorial design was used to determine the best adsorption conditions (in triplicate), to assess the influence of the pH of the RBBR dye solution (2, 6 and 10), the mass of adsorbent ( $m$ ; 1.5, 3.0 and 4.5 g), the stirring speed (VA; 50, 100 and 150 rpm) and totaling 27 assays. The levels of the variables studied are -1, 0 and +1 applied in a  $3^k$  factorial design. These assays were performed in Erlenmeyer flasks containing 100 mL of dye solution at a concentration of 50 mg L<sup>-1</sup>, which is the average output concentration found in textile plants [6]. NaOH or HCl solutions (0.1 M) were used for the pH adjustment.

In the statistical analysis of this experimental planning, Statistica 10.0 was used to apply analysis of variance (ANOVA) and the response surface methodology, thus obtaining, in response to the dye removal efficiency, a quadratic equation.

This method is a multiple regression technique used to fit a mathematical model to a set of experimental data [32].

### 2.4. Kinetic studies

Kinetic studies were performed in triplicate for a period of 32 h at 25°C in Erlenmeyer flasks containing 100 mL of dye solution (50 mg L<sup>-1</sup>) under the best conditions observed in this adsorption study. Each flask was removed from the shaker at predetermined time intervals and the samples were then immediately filtered using a vacuum pump. The final concentration of the dye in each sample was determined by reading the absorbance on a Shimadzu UV-1650 spectrophotometer, at a wavelength of 590 nm.

The kinetic data were analyzed using pseudo-first-order, pseudo-second-order, intraparticle and Elovich diffusion models.

### 2.5. Adsorption equilibrium

The adsorption equilibrium studies were similar to the adsorption kinetics studies. The experiments were conducted at temperatures of 25°C and 45°C, for the time applied in the study on the contact kinetics at concentrations of 25–150 mg L<sup>-1</sup>. After equilibration, the mixture was immediately filtered with a vacuum pump. The final concentration of the dye in each sample was determined by reading the absorbance on a Shimadzu spectrophotometer (model UV-1650), at a wavelength of 590 nm. The equilibrium study carried out at different temperatures provided information with regard to the adsorption thermodynamics. The adsorption equilibrium was assessed using the Langmuir, Freundlich, Dubinin–Radushkevich and Temkin isotherms.

## 3. Results and discussion

### 3.1. Characterization of adsorbent

#### 3.1.1. FTIR spectrometry

The presence of functional groups is of fundamental importance since many of them act as active sites for different types of adsorbates. The interaction between the functional groups and the colorant generates a decrease in the wavelength. This occurs when the dye electron withdraws a functional group

from the adsorbent [33]. The presence of a strong broad band at 3,300–3,900 cm<sup>-1</sup> may be related to the stretching frequency of the O–H groups. The region 2,800–2,890 cm<sup>-1</sup> is associated with stretching vibrations of the C–H bond, present in cellulose and hemicellulose [34]. The peaks in the region 1,100–1,000 cm<sup>-1</sup> can be assigned to the stretching vibrations of the lignin C–O bond [35]. The appearance of hydroxyl and carbonyl groups in the SBS/PET board is responsible for the interaction of the dye with the adsorbent.

#### 3.1.2. Scanning electronic microscopy

In the SEM images, it can be observed that the surface of the SBS/PET board is irregular. This SEM micrograph also shows the porous nature of the material. These porous regions are favorable to the use of SBS/PET board as an adsorbent, since they promote the adsorption of the dye. It can be observed that the cellulose fibers are more exposed due to the grinding process.

#### 3.1.3. Point of zero charge

The adsorption process is greatly affected by the surface charge of the adsorbent. Thus, the behavior of the surface charge and the manner in which it is influenced by the pH needs to be studied, since this can increase or decrease the dye-adsorbent affinity. When the pH is less than the value of pH<sub>pzc</sub> the surface of the adsorbent is protonated, favoring the adsorption of anionic dyes. On the other hand, when the pH is above the surface pH<sub>pzc</sub> the adsorbent is deprotonated (negatively charged), thus favoring the adsorption of cationic dyes [31,36]. The pH<sub>pzc</sub> of the adsorbent was determined as 7.23, indicating that the adsorbent below this value has a positive surface charge, which favors the adsorption of anions, and above this value the surface is negatively charged, facilitating the adsorption of cations. The reactive dye RBBR has several functional groups, especially sulfonated groups, which are negatively charged [6]. Thus, the interaction of the dye with the surface of the adsorbent takes place via the protonated groups of the adsorbent with the anionic groups of the dye, as corroborated by the results of the adsorption study described below.

### 3.2. Analysis of variance

The ANOVA showed that the variables, the linear terms  $X_1$ ,  $X_2$  and  $X_3$ ; interaction terms  $X_{12}$  and  $X_{13}$ ; and square terms  $X_1^2$ ,  $X_2^2$  and  $X_3^2$ , were significant with regard to the response, with a  $P$  value of <0.05 and a confidence interval of 95% (Table 1). Therefore, the linear and quadratic effects of all these variables, as well as the pH interaction with the adsorbent mass and agitation speed, were statistically significant.

The quadratic polynomial equation (Eq. (1)) obtained by applying the response surface methodology for percentage removal showed a high value for the coefficient of determination  $R^2$  (0.962), demonstrating that the model explains 96% of the process.

$$\begin{aligned} \% \text{Removal} = & 65.412 - 28.855X_1 + 11.151X_2 + 0.370X_3 \\ & - 0.552X_1X_2 + 0.005X_1X_3 + 2.203X_1^2 \\ & - 0.451X_2^2 - 0.002X_3^2 + 6.183 \end{aligned} \quad (1)$$

Table 1  
Analysis of variance (ANOVA) for the studied responses

Factor	Sum of squares	Degrees of freedom	Mean square	F Value	P Value
$X_1$	10,962.09	1	10,962.09	1,773.004	0.000000 <sup>a</sup>
$X_2$	6,786.86	1	6,786.86	1,097.705	0.000000 <sup>a</sup>
$X_3$	60.98	1	60.98	9.863	0.002735 <sup>a</sup>
$X_{12}$	701.57	1	701.57	113.472	0.000000 <sup>a</sup>
$X_{13}$	36.93	1	36.93	5.973	0.017825 <sup>a</sup>
$X_{23}$	7.96	1	7.96	1.287	0.261670
$X_{11}$	22,374.26	1	22,374.26	3,618.806	0.000000 <sup>a</sup>
$X_{22}$	58.54	1	58.54	9.469	0.003280 <sup>a</sup>
$X_{33}$	434.75	1	434.75	70.316	0.000000 <sup>a</sup>

<sup>a</sup> $P < 0.05$  with a 95% confidence interval.

### 3.2.1. Analysis of the response surface

The effect of pH on the percentage removal of RBBR and its interaction with the quantity of adsorbent are shown in Fig. 2(A). These results indicate that the maximum RBBR removal was achieved in the greater mass range and at acidic pH. The rapid increase in the adsorption as the adsorbent mass increases is attributed to an increased surface area and the availability of more active sites [37]. Fig. 2(B) shows the effect of the stirring on the percentage removal of RBBR dye. It can be observed that the maximum removal can be achieved with any stirring speed, indicating that at acidic pH the stirring has less effect on the adsorption process. Regarding the effect of pH, this behavior can be explained by the fact that under acidic conditions, hydrogen atoms ( $H^+$ ) in solution tend to protonate the surface of the adsorbent [32]. Thus, the process occurs via electrostatic interactions between the anionic dyes and the protonated groups. At low pH, more groups are protonated and an increase in the adsorption capacity occurs [38]. This behavior was also observed by Silva et al. [39], who reported that the best RBBR adsorption occurred at pH 2.0. At higher pH the negative surface of the adsorbent hinders the adsorption of the dye, due to electrostatic repulsion and excess  $OH^-$  groups, which can compete with the RBBR anions. The model predicted the removal of 76% of the RBBR at pH 2, with 4.5 g of adsorbent and a stirring speed of 100 rpm.

### 3.3. Adsorption kinetics

The adsorption kinetics were investigated in order to understand the dynamics of the adsorption process in terms of the order of the rate constant and the efficiency of the adsorbent to remove the dye [40]. Fig. 3 shows the amount of dye adsorbed on the SBS/PET board after different time intervals. The adsorption initially occurred rapidly because of the larger contact area available on the external surface and gradually decreased with time until reaching equilibrium at 10 h. The equilibrium time is similar to and/or greater than that of other materials used for the removal of the reactive dye RBBR, for example, aqueous bentonite reached equilibrium

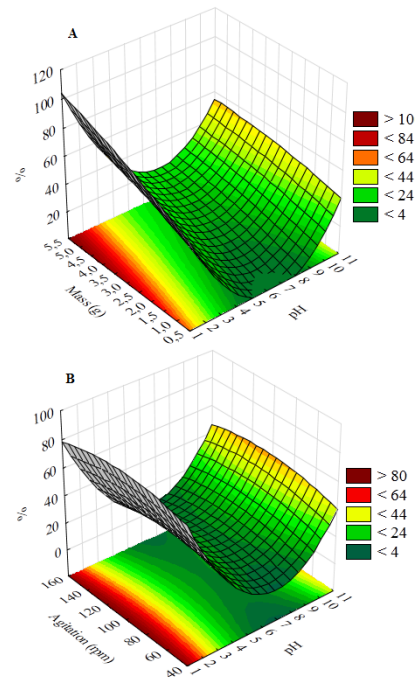


Fig. 2. Response surface showing percentage removal of RBBR: (A) pH – mass of adsorbent (g) and (B) pH – agitation (rpm).

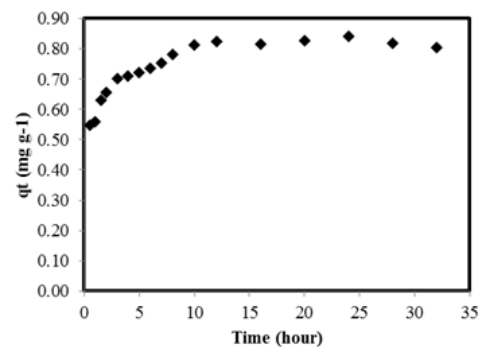


Fig. 3. Amount of reactive dye RBBR adsorbed on SBS/PET board over time.

after 120 min [41] and for orange peel the equilibration time was reported to be 15 h [42].

The pseudo-first-order, pseudo-second-order, intraparticle diffusion and Elovich kinetic models were applied to the adsorption kinetics data in order to investigate the behavior of the dye adsorption onto the SBS/PET board.

#### 3.3.1. Pseudo-first-order model

This model assumes that the solute adsorption rate over time is directly proportional to the difference in the saturation concentration and the amount of solid adsorbed over time. The pseudo-first-order model [43] is expressed by Eq. (2):

$$\frac{d q_t}{d t} = K_1(q_e - q_t) \quad (2)$$

where  $q_t$  and  $q_e$  are the quantities adsorbed ( $\text{mg g}^{-1}$ ) at time  $t$  and the equilibrium time, respectively,  $t$  is the adsorption time (min) and  $K_1$  is an adsorption rate constant ( $\text{min}^{-1}$ ). The integration of Eq. (2), applying the boundary conditions  $T = 0$ ,  $q_t = 0$  and  $t = q_t = q_e$  gives Eq. (3):

$$\log(q_e - q_t) = \log q_e - \frac{K_1}{2.303} t \quad (3)$$

From the plot of  $\log(q_e - q_t)$  vs. time  $t$ , it was possible to find the  $q$  and  $K_1$  values (Fig. 4(A)). The values of  $K_1$ ,  $R^2$  (correlation coefficient), Pearson's correlation coefficient ( $r$ ) and  $q_e$  are given in Table 2.

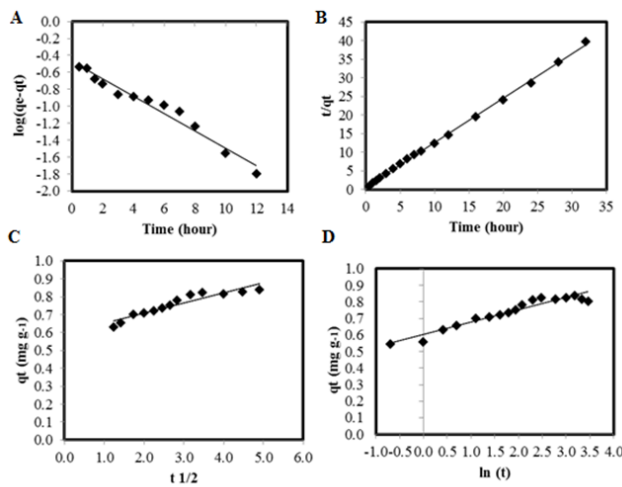


Fig. 4. (A) Pseudo-first-order kinetic model, (B) pseudo-second-order kinetic model, (C) intraparticle diffusion model and (D) Elovich model for adsorption of RBBR dye ( $50 \text{ mg L}^{-1}$ ) onto SBS/PET board.

Table 2  
Kinetic parameters for adsorption of RBBR onto SBS/PET board

Pseudo-first-order kinetic model					
$q_{e, \text{exp.}}$ ( $\text{mg g}^{-1}$ )	$q_e$ ( $\text{mg g}^{-1}$ )	$K_1$ ( $\text{min}^{-1}$ )	$R^2$	Pearson's $r$	
0.840	0.338	$2.303 \times 10^{-3}$	0.964	0.956	
Pseudo-second-order kinetic model					
$q_{e, \text{exp.}}$ ( $\text{mg g}^{-1}$ )	$q_e$ ( $\text{mg g}^{-1}$ )	$K_2$ ( $\text{g mg}^{-1} \text{min}^{-1}$ )	$h$ ( $\text{mg g}^{-1} \text{min}^{-1}$ )	$R^2$	Pearson's $r$
0.840	0.835	$3.954 \times 10^{-2}$	$2.759 \times 10^{-2}$	0.999	1.000
Intraparticle diffusion model					
$q_{e, \text{exp.}}$ ( $\text{mg g}^{-1}$ )	$C_i$ ( $\text{mg g}^{-1}$ )	$K_{\text{in}}$ ( $\text{mg g}^{-1} \text{min}^{-1/2}$ )	$R^2$	Pearson's $r$	
0.840	0.597	$7.230 \times 10^{-3}$	0.886	0.942	
Elovich model					
$q_{e, \text{exp.}}$ ( $\text{mg g}^{-1}$ )	$\alpha$ ( $\text{g g}^{-1} \text{min}^{-1}$ )	$\beta$ ( $\text{g g}^{-1}$ )	$R^2$	Pearson's $r$	
0.840	4.207	13.513	0.928	0.964	

### 3.3.2. Pseudo-second-order model

For this model, it is assumed that the adsorption capacity is proportional to the number of active sites on the adsorbent employed [44], and it is represented by Eq. (4) [45].

$$\frac{d q_t}{d t} = K_2 (q_e - q_t)^2 \quad (4)$$

Integrating Eq. (4), applying the boundary conditions  $T = 0$ ,  $q_t = 0$  and  $t = q_t = q_e$  gives Eq. (5):

$$\frac{1}{q_t} = \frac{1}{K_2 q_e^2} + \frac{1}{q_e} t \quad (5)$$

where  $K_2$  is the pseudo-second-order rate constant ( $\text{g mg}^{-1} \text{min}^{-1}$ ). The values for  $q$  and  $K_2$  can be determined from the slope and intercept of the line graph of  $t/q_t$  vs.  $t$  shown in Fig. 4(B). The initial adsorption rate [45],  $h$  ( $\text{g}^{-1} \text{mg}^{-1} \text{min}$ ), can be calculated using Eq. (6):

$$h = K_2 q_e^2 \quad (6)$$

The values for  $K_2$ , the correlation coefficient ( $R^2$ ), the Pearson's correlation coefficient ( $r$ ) and  $q_e$  are given in Table 2. The  $R^2$  and  $r$  values were 0.999 and 1.000, respectively (Table 2), suggesting a strong relationship between the parameters, indicating that the process follows pseudo-second-order kinetics. Elmoubarki et al. [2] and Isah et al. [6] observed pseudo-second-order kinetics for the adsorption of the dyes methylene blue and malachite green using clay as the adsorbent and the dye RBBR with coconut shell-based activated carbon, respectively.

### 3.3.3. Intraparticle diffusion model

The dye transport to the surface of the adsorbent particles takes place in three stages (film diffusion, intraparticle diffusion and saturation). First, the dye migrates through the solution to the outer surface of the adsorbent particles. Second, the dye moves into the pores of the particles and third, it is absorbed at sites on the interior surface of the adsorbent particles. This phase occurs very rapidly and does not represent a rate-limiting step in the dye adsorption onto the waste material [46]. The intraparticle diffusion model is expressed by Eq. (7):

$$q_t = K_{in} t^{1/2} + C_i \quad (7)$$

where  $K_{in}$  is the intraparticle diffusion constant ( $\text{mg g}^{-1} \text{min}^{-1/2}$ ) and  $C_i$  is a constant related to the diffusion resistance. The  $K_{in}$  values and  $C_i$  can be determined from the slope and intercept of the line graph of  $q_t$  vs.  $t^{1/2}$  shown in Fig. 4(C). The values for  $K_{in}$ ,  $R^2$  (correlation coefficient), Pearson's  $r$  (correlation coefficient) and  $C_i$  are given in Table 2.

### 3.3.4. Elovich model

The Elovich equation is one of chemical equations most commonly used to describe the adsorption kinetics of a dye onto the surface of SBS/PET board [47,48]. A modified form of the Elovich model is expressed by Eq. (8):

$$q_t = \frac{1}{\beta} \ln(\alpha\beta) + \left(\frac{1}{\beta}\right) \ln(t) \quad (8)$$

where  $\alpha$  and  $\beta$  are constants:  $\alpha$  being the initial rate of adsorption ( $\text{g g}^{-1} \text{min}^{-1}$ ) and  $\beta$  the adsorption constant ( $\text{g g}^{-1}$ ).

The  $\alpha$  and  $\beta$  values can be determined from the slope and intercept of the line graph of  $q_t$  vs.  $\ln(t)$  shown in Fig. 4(D). The values for  $\alpha$ ,  $\beta$ ,  $R^2$  (correlation coefficient) and the Pearson's  $r$  (correlation coefficient) are given in Table 2.

### 3.4. Adsorption isotherms

The adsorption isotherms are used to develop a model that can be used to describe the adsorption process [49]. The equilibrium data for the adsorption of RBBR with SBS/PET board were assembled using the Langmuir, Freundlich, Temkin and Dubinin–Radushkevich adsorption isotherms.

The Langmuir isotherm is the simplest theoretical model and it assumes a monolayer adsorption onto a surface with a finite number of identical active sites. The equation is applicable to homogeneous adsorption, where the adsorption process has the same activation energy. The adsorption isotherm of Langmuir [50] is represented by Eq. (9):

$$q_e = \frac{q_m K_L C_0}{1 + K_L C} \quad (9)$$

where  $C$  ( $\text{mg L}^{-1}$ ) and  $q_e$  ( $\text{g}^{-1} \text{mg}$ ) are the concentration of the liquid phase and the concentration of the solid phase of the adsorbate at equilibrium, respectively,  $q_m$  ( $\text{mg g}^{-1}$ ) is the maximum adsorption capacity of the adsorbent and  $K_L$  ( $\text{L mg}^{-1}$ ) is the constant of the Langmuir model.

The parameters calculated from the Langmuir model are shown in Table 3. The Langmuir constant,  $q_m$ , represents the monolayer adsorption capacity and for the SBS/PET board its values were 1.527, and 0.928  $\text{mg g}^{-1}$  for temperatures of 298 and 315 K, respectively. These  $q_m$  values are lower than those reported for biosorbents based on other materials, such as,

Table 3  
Isothermal parameters and regression coefficients at different temperatures for RBBR adsorption onto SBS/PET board

Temperature (K)	Langmuir model				
	$q_m$ ( $\text{mg g}^{-1}$ )	$K_L$ ( $\text{L mg}^{-1}$ )	$R_L$	$R^2$	Pearson's $r$
298	1.527	0.099	0.134	0.985	0.993
315	0.928	0.123	0.112	0.973	0.991
	Freundlich model				
	$K_f$ ( $\text{mg}^{1-1/n} \text{L}^{1/n} \text{g}^{-1}$ )	$1/n$	$n$	$R^2$	Pearson's $r$
298	0.378	0.298	3.356	0.995	0.998
315	0.340	0.206	4.856	0.995	0.944
	Temkin model				
	$A$ ( $\text{L mg}^{-1}$ )	$b$ ( $\text{J g mg}^{-1} \text{mol}^{-1}$ )	$B$ ( $\text{mg g}^{-1}$ )	$R^2$	Pearson's $r$
298	2.216	9,529.120	0.260	0.980	0.990
315	6.958	20,029.180	0.132	0.898	0.948
	Dubinin–Radushkevich model				
	$k_d$ ( $\text{kmol}^2 \text{J}^{-2}$ )	$q_m$ ( $\text{mg g}^{-1}$ )	$E$ ( $\text{kJ mol}^{-1}$ )	$R^2$	Pearson's $r$
298	0.001	1.154	22.360	0.798	0.893
315	0.003	0.805	12.901	0.887	0.942

laundry sewage sludge ( $q_m$  of 33.47 mg g<sup>-1</sup>) [39], orange peel ( $q_m$  of 11.62 mg g<sup>-1</sup>) [42] and coconut shell ( $q_m$  of 2.22 mg g<sup>-1</sup>) [6]. It should be noted that the adsorption capacity of adsorbents can vary significantly depending on the characteristics of the adsorbent, the extent of chemical modification and the dye concentration.

The Langmuir constant,  $K_L$ , which indicates the energy of adsorption, was 0.099 L mg<sup>-1</sup> at 298 K and increased with increases in the temperature (Table 3). The equilibrium parameter  $R_L$  was applied to reveal the type of isotherm, as defined by Eq. (10):

$$R_L = \frac{1}{1 + K_L C_0} \quad (10)$$

where  $C_0$  is the initial concentration (mg L<sup>-1</sup>) and  $K_L$  (L mg<sup>-1</sup>) is the constant of the Langmuir model. The  $R_L$  value indicates the adsorption behavior as follows:  $R_L > 1$  (unfavorable),  $R_L = 1$  (linear),  $1 < R_L < 0$  (favorable) and  $R_L = 0$  (irreversible) [51]. In this study, the  $R_L$  values calculated were in the range of  $1 < R_L < 0$  (Table 3), which indicates that the SBS/PET board is adequate for the adsorption of RBBR dye and the adsorption process is favorable. The Freundlich isotherm represented by Eq. (11) is an empirical equation that assumes heterogeneous adsorption due to the variety of active adsorption sites [52]:

$$q_e = K_f C^{1/n} \quad (11)$$

where  $q_e$  (mg g<sup>-1</sup>) is the adsorption capacity at equilibrium,  $K_f$  is the Freundlich constant,  $C$  is the concentration of adsorbate in solution (mg L<sup>-1</sup>) and  $1/n$  indicates the type of isotherm as follows: irreversible ( $1/n = 0$ ), positive ( $0 < 1/n < 1$ ) and unfavorable ( $1/n > 1$ ) [53]. The parameters calculated from the Freundlich model are shown in Table 3.

The results showed that the experimental data are consistent with the Freundlich model, confirming the values for Pearson's  $r$  and  $R^2$  of 0.944 and 0.995, respectively (Table 3). The Freundlich model describes the nature of the heterogeneity of the active sites of the dye molecules involved in the adsorbent surface interactions [6]. The values calculated for  $1/n$  were in the range of  $0 < 1/n < 1$  (Table 3), which indicates that the SBS/PET board was suitable for the adsorption of RBBR dye and the adsorption process is favorable.

Temkin and Pyzhev considered the effects of indirect interactions between the adsorbate and the adsorbent. The heat of adsorption of all the molecules in the layer decreases linearly according to the height of the layer of the adsorbent due to interaction with the adsorbate [54]. Temkin's model can be expressed by Eq. (12):

$$q_e = \left( \frac{RT}{b} \right) \ln(AC_e) \quad (12)$$

where  $RT/b = B$  is related to the adsorption heat,  $R$  is the gas constant (8.31 J mol<sup>-1</sup> K<sup>-1</sup>),  $T$  (K) is the absolute temperature and  $A$  is the binding constant, which corresponds to the maximum equilibrium binding energy. The constants  $A$  and  $B$  together with the values of Pearson's  $r$  and  $R^2$  are given in Table 3.

The Dubinin–Radushkevich isotherm is an empirical model initially considered for the adsorption of subcritical vapors onto microporous solids and commonly applied to express an adsorption mechanism with a Gaussian energy distribution on a heterogeneous surface [55]. The linear shape of the Dubinin–Radushkevich model can be represented by Eq. (13):

$$\ln q_e = \ln Q_m - k_d \varepsilon^2 \quad (13)$$

where  $q_e$  (mg g<sup>-1</sup>) is the amount of RBBR adsorbed per unit mass of adsorbent,  $k_d$  (mol<sup>2</sup> J<sup>-2</sup>) is a constant that relates to the energy of the adsorption system,  $Q_m$  (mg g<sup>-1</sup>) is the theoretical adsorption capacity and  $\varepsilon$  is the Polanyi potential, which can be calculated according to Eq. (14):

$$\varepsilon = RT \ln \left( 1 + \frac{1}{C} \right) \quad (14)$$

where  $R$  is the gas constant (8.31 J mol<sup>-1</sup> K<sup>-1</sup>) and  $T$  is the temperature (K). The values for the isotherm constants ( $Q_m$  and  $k_d$ ) are defined from the intercept and slope of the linear graph of  $\ln q_e$  against  $\varepsilon^2$ , respectively. The mean free energy of adsorption ( $E$ ) for the transfer of 1 mol of target from infinity in solution to the solid surface was calculated from the  $k_d$  value using Eq. (15):

$$E = \frac{1}{\sqrt{2k_d}} \quad (15)$$

The value of  $E$  (kJ mol<sup>-1</sup>) provides information on the type of adsorption, that is, physical or chemical. When  $E < 8$  kJ mol<sup>-1</sup>, the adsorption process is physical, at 8–16 kJ mol<sup>-1</sup> a chemical ion-exchange process occurs, and at 20–40 kJ mol<sup>-1</sup> the process is chemical in nature [55,56]. The parameters calculated from the Dubinin–Radushkevich model are shown in Table 3. The  $E$  values were 22.360, and 12.909 kJ mol<sup>-1</sup> for temperatures of 298 and 315 K, which indicates chemical and ion-exchange adsorption process, respectively.

In Fig. 5, it can be verified that the experimental data are in agreement with the isothermal models, especially the Freundlich model, which provided higher values for the Pearson's  $r$  and  $R^2$  when compared with the Langmuir,

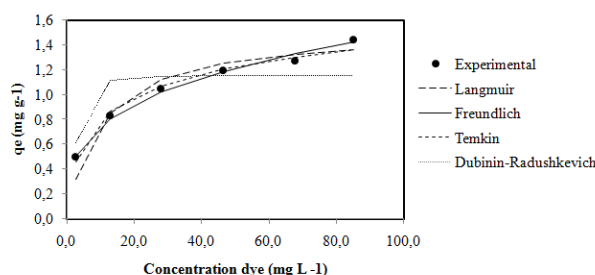


Fig. 5. Amount of dye adsorbed at 298 K according to data obtained experimentally and applying the Langmuir, Freundlich, Temkin and Dubinin–Radushkevich models.

Temkin and Dubinin–Radushkevich models (Table 3), and thus best describes the adsorption data. According to the results obtained, the suitability of the isothermal models for describing the adsorption of RBBR onto SBS/PET board decreased in the following order: Freundlich > Langmuir > Temkin > Dubinin–Radushkevich, at both temperatures.

The Freundlich model, which provided excellent results in this study, also reportedly provided the best fit for the adsorption of the dyes Blue Remazol R160, Rubi S2G, Red Remazol 5R, Violet Remazol 5R and Indanthrene Olive Green onto coconut bagasse [57] and the adsorption of the dye RBBR onto coconut shell-based activated carbon [6].

### 3.5. Adsorption thermodynamics

The thermodynamic parameters [49] in the form of the Gibbs free energy ( $\Delta G^\circ$ ), enthalpy ( $\Delta H^\circ$ ) and entropy ( $\Delta S^\circ$ ) were calculated using Eqs. (16)–(18).

$$\Delta G^\circ = RT \ln K_c \quad (16)$$

$$K_c = \frac{q_e}{C_e} \quad (17)$$

$$\ln K_c = \frac{\Delta S^\circ}{R} - \frac{\Delta H^\circ}{RT} \quad (18)$$

where  $R$  (8.314 J mol<sup>-1</sup> K<sup>-1</sup>) is the gas constant,  $T$  (K) is the absolute temperature of the solution and  $K_c$  (L g<sup>-1</sup>) is the thermodynamic equilibrium constant defined by  $q_e/C_e$ .

The values for  $\Delta H^\circ$  and  $\Delta S^\circ$ , defined from the intercept and the slope of the linear plot of  $\ln K_c$  vs.  $1/T$ , respectively, are shown in Table 4. When  $\Delta G^\circ$  is positive the reverse reaction is spontaneous, when  $\Delta G^\circ$  is negative the reaction is spontaneously forward, and when  $\Delta G^\circ$  is zero the system reached a steady state. Positive  $\Delta G^\circ$  values indicate that the adsorption process leads to an increase in the Gibbs free energy [41]. On the other hand, negative  $\Delta H^\circ$  values indicate that the process is exothermic in nature, and negative  $\Delta S^\circ$  values mean that the dye molecules at the solid–liquid interface are more organized than those in the bulk solution phase [58].

The values for  $\Delta G^\circ$ ,  $\Delta H^\circ$  and  $\Delta S^\circ$  indicate that the process is of a non-spontaneous exothermic nature for the adsorption of the dye RBBR onto SBS/PET board (Table 4). The  $\Delta H^\circ$  and  $\Delta S^\circ$  data obtained showed the same thermodynamic behavior previously observed in the adsorption of an anionic dye (Reactive Red 120) onto natural clay [58]. The behavior of  $\Delta G^\circ$  was similar to that observed in a study on the adsorption of an aqueous solution of the dye RBBR by bentonite [41].

## 4. Conclusions

The results reported herein verify that SBS paper-board coated with PET exhibits adsorption properties and can be recommended as a material for the removal of the dye RBBR from solution. The variables considered and the levels employed in this study were effective in demonstrating the percentage removal of this dye. The experimental design indicated that the concentration of

Table 4

Thermodynamic parameters of RBBR dye adsorption onto SBS/PET board at different temperatures

Concentration (mg L <sup>-1</sup> )	Thermodynamic parameters			
	$\Delta H^\circ$ (kJ mol <sup>-1</sup> )	$\Delta S^\circ$ (J mol <sup>-1</sup> K <sup>-1</sup> )	$\Delta G^\circ$ (kJ mol <sup>-1</sup> )	
			298 K	315 K
25	-29.515	-112.821	4.141	6.382
50	-19.538	-88.295	6.790	8.543
75	-27.902	-120.886	8.134	10.534
100	-36.640	-143.998	9.077	11.937
125	-24.701	-115.897	9.847	12.147
150	-28.201	-128.451	10.108	12.658

adsorbent and the pH have an important influence on the adsorption of RBBR onto SBS/PET board. The model obtained indicates that higher removal percentages are achieved on applying acidic pH, higher concentrations of adsorbent and moderate stirring. Of the models tested, the pseudo-second-order model described more accurately the adsorption kinetics for the adsorption of the reactive dye RBBR onto SBS/PET board, which reached equilibrium after 10 h. The maximum adsorption capacity for the dye RBBR was estimated to be 1,527 mg dye per g adsorbent at 298 K. The Freundlich model best described the adsorption data, proving higher Pearson's  $r$  and the  $R^2$  values. The thermodynamic study indicated that the dye adsorption is an exothermic process, suggesting more favorable adsorption at room temperature.

## Symbols

$A$	—	Maximum equilibrium binding energy, L mg <sup>-1</sup>
$\alpha$	—	Initial rate of adsorption, g g <sup>-1</sup> min <sup>-1</sup>
$B$	—	Adsorption heat, mg g <sup>-1</sup>
$\beta$	—	Adsorption constant, g g <sup>-1</sup>
$C_t$	—	Concentration at time $t$ , mg L <sup>-1</sup>
$C$	—	Concentration of adsorbate in solution, mg L <sup>-1</sup>
$C_i$	—	Constant related to the diffusion resistance
$C_0$	—	Initial concentration of the compound, mg L <sup>-1</sup>
$E$	—	Mean free energy of adsorption, kJ mol <sup>-1</sup>
$\varepsilon$	—	Polanyi potential
$h$	—	Initial adsorption rate, g <sup>-1</sup> mg <sup>-1</sup> min
$K$	—	Kelvin
$K_1$	—	Adsorption rate constant, min <sup>-1</sup>
$K_L$	—	Constant of the Langmuir isotherm, L mg <sup>-1</sup>
$k_d$	—	Constant that relates to the energy of the absorption system, mol <sup>2</sup> J <sup>-2</sup>
$K_f$	—	Freundlich constant, mg <sup>1-1/n</sup> L <sup>1/n</sup> g <sup>-1</sup>
$K_{in}$	—	Intraparticle diffusion constant, mg g <sup>-1</sup> min <sup>-1/2</sup>
$K_2$	—	Pseudo-second-order constant, g mg <sup>-1</sup> min <sup>-1</sup>
$K_c$	—	Thermodynamic equilibrium constant, L g <sup>-1</sup>
$m$	—	Mass of adsorbent, g
$V$	—	Solution volume, L
$q_m$	—	Maximum adsorption capacity of the adsorbent, mg g <sup>-1</sup>
$q_t$	—	Quantity adsorbed at time $t$ , mg g <sup>-1</sup>
$q_e$	—	Quantity adsorbed at equilibrium, mg g <sup>-1</sup>

$Q_m$	—	Theoretical adsorption capacity, mg g <sup>-1</sup>
$R$	—	Gas constant, mol <sup>-1</sup> K <sup>-1</sup>
RBRR	—	Remazol Brilliant Blue Reactive
$R_L$	—	Langmuir equilibrium parameter
$T$	—	Temperature, K
$t$	—	Adsorption time, min
$\Delta H^\circ$	—	Adsorption enthalpy, kJ mol <sup>-1</sup>
$\Delta S^\circ$	—	Entropy, J mol <sup>-1</sup> K <sup>-1</sup>
$\Delta G^\circ$	—	Gibbs free energy, kJ mol <sup>-1</sup>

## References

- [1] A.T. Ansari, N. Sundaramoorthy, M. Kavitha, Adsorption, biosorption and discolourisation of rhodamine-B and basic violet-2 using fungi isolated from soil samples collected near textile dye industry, *J. Pharm. Biomed. Sci.*, 6 (2011) 1706–1710.
- [2] R. Elmoubarki, F.Z. Mahjoubi, H. Tounsadi, J. Moustadraf, M. Abdennouri, A. Zouhri, A. Albani, N. Barka, Adsorption of textile dyes on raw and decanted Moroccan clays: kinetics, equilibrium and thermodynamics, *Water Resour. Ind.*, 9 (2015) 16–29.
- [3] M. Sathiyar, S. Periyar, A. Sasikalaveni, K. Murugesan, P.T. Kalaiichelvan, Decolorization of textile dyes and their effluents using white rot fungi, *Afr. J. Biotechnol.*, 9 (2007) 424–429.
- [4] H. Parab, M. Sudersanan, N. Shenoy, T. Pathare, B. Vaze, Use of agro-industrial wastes for removal of basic dyes from aqueous solutions, *Clean Soil Air Water*, 37 (2009) 963–969.
- [5] Z. Aksu, S. Tezer, Biosorption of reactive dyes on the green alga *Chlorella vulgaris*, *Process Biochem.*, 40 (2005) 1347–1361.
- [6] U. Isah, G. Abdulraheem, S. Bala, S. Muhammad, M. Abdullahi, Kinetics, equilibrium and thermodynamics studies of CI Reactive Blue 19 dye adsorption on coconut shell based activated carbon, *Int. Biodeterior. Biodegrad.*, 102 (2015) 265–273.
- [7] T. Hadibarata, A.R.M. Yusoff, R.A. Kristanti, Decolorization and metabolism of anthraquinone-type dye by laccase of white-rot fungi *Polyporus* sp. S133, *Water Air Soil Pollut.*, 223 (212) 933–941.
- [8] N.N. Sing, A. Husaini, A. Zulkharnain, H.A. Roslan, Decolourisation capabilities of ligninolytic enzymes produced by *Marasmius cladophyllus* UMAS MS8 on remazol brilliant blue R and other azo dyes, *Biomed. Res. Int.*, 2017 (2017) 1–8.
- [9] F.N. Memon, S. Memon, Calixarenes: a versatile source for the recovery of Reactive Blue-19 dye from industrial wastewater, *Pak. J. Anal. Environ. Chem.*, 13 (2012) 148–158.
- [10] M. Asgher, S. Kausar, H.N. Bhatti, S.A.H. Shah, M. Ali, Optimization of medium for decolorization of Solar golden yellow R direct textile dye by *Schizophyllum commune* IBL-06, *Int. Biodeterior. Biodegrad.*, 61 (2008) 189–193.
- [11] A.K. Sarkar, A. Pal, S. Ghorai, N.R. Mandre, S. Pal, Efficient removal of malachite green dye using biodegradable graft copolymer derived from amylopectin and poly(acrylic acid), *Carbohydr. Polym.*, 111 (2014) 108–115.
- [12] E. Lorenc-Grabowska, M.A. Diez, G. Gryglewicz, Influence of pore size distribution on the adsorption of phenol on PET-based activated carbons, *J. Colloid Interface Sci.*, 469 (2016) 205–212.
- [13] J. Mittal, A. Mittal, H. Feather, Hen Feather: A Remarkable Adsorbent for Dye Removal, S.K. Sharma, Ed., A Remarkable Adsorbent for Dye Removal, Green Chemistry for Dyes Removal from Wastewater, Vol. 11, Scrivener Publishing LLC, USA, 2015, pp. 409–457.
- [14] C. Namasivayam, D. Sangeetha, Recycling of agricultural solid waste, coir pith: removal of anions, heavy metals, organics and dyes from water by adsorption onto ZnCl<sub>2</sub> activated coir pith carbon, *J. Hazard. Mater.*, 135 (2006) 449–452.
- [15] A. Mittal, R. Ahmad, I. Hasan, Iron oxide-impregnated dextrin nanocomposite: synthesis and its application for the biosorption of Cr(VI) ions from aqueous solution, *Desal. Wat. Treat.*, 57 (2016) 15133–15145.
- [16] A. Mittal, R. Ahmad, I. Hasan, Biosorption of Pb<sup>2+</sup>, Ni<sup>2+</sup> and Cu<sup>2+</sup> ions from aqueous solutions by L-cystein-modified montmorillonite-immobilized alginate nanocomposite, *Desal. Wat. Treat.*, 57 (2016) 17790–17807.
- [17] A. Mittal, R. Ahmad, I. Hasan, Poly (methyl methacrylate)-grafted alginate/Fe<sub>3</sub>O<sub>4</sub> nanocomposite: synthesis and its application for the removal of heavy metal ions, *Desal. Wat. Treat.*, 57 (2016) 19820–19833.
- [18] A. Mittal, M. Naushad, G. Sharma, Z.A. AlOthman, S.M. Wabaidur, M. Alam, Fabrication of MWCNTs/ThO<sub>2</sub> nanocomposite and its adsorption behavior for the removal of Pb(II) metal from aqueous medium, *Desal. Wat. Treat.*, 57 (2016) 21863–21869.
- [19] R. Ahmad, I. Hasan, A. Mittal, Adsorption of Cr(VI) and Cd(II) on chitosan grafted polyaniline-OMMT nanocomposite: isotherms, kinetics and thermodynamics studies, *Desal. Wat. Treat.*, 58 (2017) 144–153.
- [20] A. Mittal, M. Teotia, R.K. Soni, J. Mittal, Applications of egg shell and egg shell membrane as adsorbents: a review, *J. Mol. Liq.*, 223 (2016) 376–387.
- [21] G. Sharma, M. Naushad, D. Pathania, A. Mittal, G.E. El-Desoky, Modification of *Hibiscus cannabinus* fiber by graft copolymerization: application for dye removal, *Desal. Wat. Treat.*, 54 (2015) 3114–3121.
- [22] S. Chowdhury, R. Mishra, P. Saha, P. Kushwaha, Adsorption thermo-dynamics, kinetics and isosteric heat of adsorption of malachite green onto chemically modified rice husk, *Desalination*, 265 (2011) 159–168.
- [23] L. Zhou, J. Huang, B. He, F. Zhang, H. Li, Peach gum for efficient removal of methylene blue and methyl violet dye from aqueous solution, *Carbohydr. Polym.*, 101 (2014) 574–581.
- [24] K.G. Bhattacharyya, A. Sharma, *Azadirachta indica* leaf powder as an effective biosorbent for dyes: a case study with aqueous congo red solutions, *J. Environ. Manage.*, 71 (2004) 217–229.
- [25] U. Garg, M.P. Kaur, V.K. Garg, D. Sud, Removal of hexavalent chromium from aqueous solution by agricultural waste biomass, *J. Hazard. Mater.*, 140 (2007) 60–68.
- [26] T. Robinson, B. Chandran, P. Nigam, Effect of pretreatments of three waste residues, wheat straw, corncobs and barley husks on dye adsorption, *Bioresour. Technol.*, 85 (2002) 119–124.
- [27] A. Mital, L. Kurup, Column operations for the removal and recovery of a hazardous dye 'Acid Red-27' from aqueous solutions, using waste materials-bottom ash and de-oiled soya, *Ecol. Environ. Conserv. Pap.*, 13 (2006) 181–186.
- [28] Z.M. Magriotis, S.S. Vieira, A.A. Saczk, N.A. Santos, N.R. Stradiotto, Removal of dyes by lignocellulose adsorbents originating from biodiesel production, *J. Environ. Chem. Eng.*, 2 (2014) 2199–2210.
- [29] A. Drewnowski, Fat and sugar: an economic analysis, *J. Nutr.*, 133 (2003) 1–3.
- [30] A. Ness, Diet, nutrition and the prevention of chronic diseases, WHO Technical Report Series 916, Report of a Joint WHO/FSA Expert Consultation, *Int. J. Epidemiol.*, 33 (2004) 914–915.
- [31] M.R. Awwal, M.M. Hasan, T. Ihara, T. Yaita, Mesoporous silica based novel conjugate adsorbent for efficient selenium(IV) detection and removal from water, *Microporous Mesoporous Mater.*, 197 (2014) 331–338.
- [32] D. Baş, I. H. Boyacı, Modeling and optimization I: usability of response surface methodology, *J. Food Eng.*, 78 (2007) 836–845.
- [33] N.F. Cardoso, E.C. Lima, T. Calvete, I.S. Pinto, C.V. Amavisca, T.H. Fernandes, B.R. Pinto, W.S. Alencar, Application of acai stalks as biosorbents for the removal of the dyes Reactive Black 5 and Reactive Orange 16 from aqueous solution, *J. Chem. Eng. Data*, 56 (2011) 1857–1868.
- [34] H. Yang, R. Yan, H. Chen, D.H. Lee, C. Zheng, Characteristics of hemicellulose, cellulose and lignin pyrolysis, *Fuel*, 86 (2007) 1781–1788.
- [35] N.F. Cardoso, R.B. Pinto, E.C. Lima, T. Calvete, C.V. Amavisca, B. Royer, M.L. Cunha, T.H.M. Fernandes, I.S. Pinto, Removal of remazol black B textile dye from aqueous solution by adsorption, *Desalination*, 269 (2011) 92–103.
- [36] D. Dayananda V.R. Sarva, S.V. Prasad, J. Arunachalam, N.N. Ghosh, Preparation of CaO loaded mesoporous Al<sub>2</sub>O<sub>3</sub>: efficient adsorbent for fluoride removal from water, *Chem. Eng. J.*, 248 (2014) 430–439.
- [37] M. Dastkhooon, M. Ghaedi, A. Asfaram, A. Goudarzi, S.M. Langroodi, I. Tyagi, S. Agarwal, V.K. Gupta, Ultrasound

- assisted adsorption of malachite green dye onto ZnS:Cu-NP-AC: equilibrium isotherms and kinetic studies – response surface optimization, *Sep. Purif. Technol.*, 156 (2015) 780–788.
- [38] T.V. Rêgo, T.R.S. Cadaval, G.L. Dotto, L.A.A. Pinto, Statistical optimization, interaction analysis and desorption studies for the azo dyes adsorption onto chitosan films, *J. Colloid Interface Sci.*, 411 (2013) 27–33.
- [39] T.L. Silva, A. Ronix, O. Pezoti, L.S. Souza, P.K. Leandro, K.C. Bedin, K.K. Beltrame, A.L. Cazetta, V.C. Almeida, Mesoporous activated carbon from industrial laundry sewage sludge: adsorption studies of reactive dye Remazol Brilliant Blue R, *Chem. Eng. J.*, 303 (2016) 467–476.
- [40] H. Nourmoradia, M. Nikaeena, M. Khiadani, Removal of benzene, toluene, ethylbenzene and xylene (BTEX) from aqueous solutions by montmorillonite modified with nonionic surfactant: equilibrium, kinetic and thermodynamic study, *Chem. Eng. J.*, 191 (2012) 341–348.
- [41] K. Chinoune, K. Bentaleb, Z. Boubberka, A. Nadim, U. Maschke, Adsorption of reactive dyes from aqueous solution by dirty bentonite, *Appl. Clay Sci.*, 123 (2016) 64–75.
- [42] M.R. Mafra, L. Igarashi-Mafra, D.R. Zuim, É.C. Vasques, M.A. Ferreira, Adsorption of remazol brilliant blue on an orange peel adsorbent, *Braz. J. Chem. Eng.*, 30 (2013) 657–665.
- [43] A. Hosseini-Bandegharai, M.S. Hosseini, M. Sarw-Ghadi, S. Zowghi, E. Hosseini, H. Hosseini-Bandegharai, Kinetics, equilibrium and thermodynamic study of Cr(VI) sorption into toluidine blue o impregnated XAD-7 resin beads and its application for the treatment of wastewaters containing Cr(VI), *Chem. Eng. J.*, 160 (2010) 190–198.
- [44] M. Uğurlu, M.H. Karaoğlu, Adsorption of ammonium from an aqueous solution by fly ash and sepiolite: isotherm, kinetic and thermodynamic analysis, *Microporous Mesoporous Mater.*, 139 (2011) 173–178.
- [45] Y.S. Ho, G. McKay, Pseudo-second order model for sorption processes, *Process Biochem.*, 34 (1999) 451–465.
- [46] S.J. Allen, G. McKay, K.Y.H. Khader, Intraparticle diffusion of a basic dye during adsorption onto sphagnum peat, *Environ. Pollut.*, 56 (1989) 39–50.
- [47] H.I. Inyang, A. Onwawoma, S. Bae, The Elovich equation as a predictor of lead and cadmium sorption rates on contaminant barrier minerals, *Soil Tillage Res.*, 155 (2016) 124–132.
- [48] F.C. Wu, R.L. Tseng, R.S. Juang, Characteristics of Elovich equation used for the analysis of adsorption kinetics in dye-chitosan systems, *Chem. Eng. J.*, 150 (2009) 366–373.
- [49] Q. Li, Q.Y. Yue, Y. Su, B.Y. Gao, H.J. Sun, Equilibrium, thermodynamics and process design to minimize adsorbent amount for the adsorption of acid dyes onto cationic polymer-loaded bentonite, *Chem. Eng. J.*, 158 (2010) 489–497.
- [50] J. Rahchamani, H.Z. Mousavi, M. Behzad, Adsorption of methyl violet from aqueous solution by polyacrylamide as an adsorbent: isotherm and kinetic studies, *Desalination*, 267 (2011) 256–260.
- [51] C.H. Huang, K.P. Chang, H.D. Ou, Y.C. Chiang, C.F. Wang, Adsorption of cationic dyes onto mesoporous silica, *Microporous Mesoporous Mater.*, 141 (2011) 102.
- [52] Y.C. Chiang, P.Y. Wu, Adsorption equilibrium of sulfur hexafluoride on multi-walled carbon nanotubes, *J. Hazard. Mater.*, 178 (2010) 729–738.
- [53] K. Nuithitikul, S. Srikhun, S. Hirunpraditkoon, Kinetics and equilibrium adsorption of Basic Green 4 dye on activated carbon derived from durian peel: effects of pyrolysis and post-treatment conditions, *J. Taiwan Inst. Chem. Eng.*, 41 (2010) 591–598.
- [54] I.A.W. Tan, A.L. Ahmad, B.H. Hameed, Adsorption of basic dye on high-surface-area activated carbon prepared from coconut husk: equilibrium, kinetic and thermodynamic studies, *J. Hazard. Mater.*, 154 (2008) 337–346.
- [55] S. Agarwal, I. Tyagi, V.K. Gupta, S. Mashhadi, M. Ghasemi, Kinetics and thermodynamics of Malachite Green dye removal from aqueous phase using iron nanoparticles loaded on ash, *J. Mol. Liq.*, 223 (2016) 1340–1347.
- [56] M. Ghasemi, S. Mashhadi, M. Asif, I. Tyagi, S. Agarwal, V.K. Gupta, Microwave-assisted synthesis of tetraethylenepentamine functionalized activated carbon with high adsorption capacity for Malachite green dye, *J. Mol. Liq.*, 213 (2016) 317–325.
- [57] A.P. Vieira, S.A. Santana, C.W. Bezerra, H.A. Silva, J.A. Chaves, J.C. de Melo, E.C. da S. Filho, C. Airoidi, Kinetics and thermodynamics of textile dye adsorption from aqueous solutions using babassu coconut mesocarp, *J. Hazard. Mater.*, 166 (2009) 1272–1278.
- [58] E. Errais, J. Duplay, F. Darragi, I. M'Rabet, A. Aubert, F. Huber, G. Morvan, Efficient anionic dye adsorption on natural untreated clay: kinetic study and thermodynamic parameters, *Desalination*, 275 (2011) 74–81.